IEEE Access
Multidisciplinary | Rapid Review | Open Access Journal

Received May 19, 2020, accepted June 2, 2020, date of publication June 5, 2020, date of current version June 16, 2020.

Digital Object Identifier 10.1109/ACCESS.2020.3000360

Direction-of-Arrival Estimation in a Mixture of Multiple Circular and Non-Circular Signals Using Nested Array

PENG HAN, HAIYUN XU, BIN BA, AND YANKUI ZHANG
National Digital Switching System Engineering and Technological Research Center, Zhengzhou 450001, China
Corresponding author: Peng Han (sunrisehp@163.com)

This work was supported in part by the National Natural Science Foundation of China under Grant 61401513.

ABSTRACT In practice, there are many circular and non-circular signals due to multipath propagation and various modulations. Conventional direction-of-arrival (DOA) estimation in a mixture of circular and non-circular signals cannot distinguish two kind of signals and detect more sources than number of sensors at the same time. This paper proposes a novel separation algorithm based on elliptic covariance matrix (ECM) which possesses accurate DOA estimation and high degrees of freedom (DOF) with low complexity. Firstly it estimates non-circular signals using ECM which contains non-circular information merely. Considering that the virtual array generated from nested array using ECM is inconsecutive, a matrix completion method via nuclear norm minimization is also included and as a result, the freedom degrees are further extended. On the basis of ECM, the paper also introduces a separation algorithm through subtraction of two reconstructed Toeplitz covariance matrix (CM). Detailed analysis and theoretically proof is presented subsequently and DOAs of circular signals can be obtained after separation. Simulation results show that the proposed algorithm can realize underdetermined estimation and get accurate DOAs while two kind of signals are separated simultaneously.

INDEX TERMS Direction-of-arrival, nested array, non-circular signals, separation technique, matrix completion.

I. INTRODUCTION

Direction-of-arrival estimation is a significant problem in array signal processing [1]. It is also an important signal metric in target localization based on antenna array [2], [3]. DOA estimation has been studied extensively since multiple signal classification (MUSIC) [4] was proposed in 1986. In addition, researchers have developed numerous high-resolution algorithms like estimating signal parameters via rotational invariance techniques (ESPRIT) [5], propagator method [6] and so forth. However, these traditional algorithms have not considered properties of the impinging sources.

Recently, several works considering about non-circularity have been proposed to utilize more available information. The array output data can be expanded by combining received data vector and its conjugate together. Thus, the array aperture and degrees of freedom can get great improvement. Moreover, P. Gupta developed a method for non-circular signals estimation based on fourth order cumulant [7]. Other researchers studied the effect which multipath propagation projects on DOA estimation and proposed an efficient method for coherent non-circular signals [8]. Many studies related to non-circular signals have been proposed, but they cannot obtain high accuracy as well as underdetermined DOA estimation at the same time. Various uniform arrays are used in these algorithms, which might be affected by mutual coupling error and cause worse performance. Although some researchers developed a DOA estimation method which can calibrate mutual coupling error [9], it was hard for promotion and was difficult to be widely used. Besides, the resolution capability and degrees of freedom of half wave length spaced uniform linear arrays (ULA) is greatly limited by the number of antenna array sensors.

As a result, sparse array becomes a better choice for DOA estimation based on antenna array. Shi *et al.* developed a DOA estimation method using sparse representation based on coprime array [10]. Besides, a virtual array interpolation method dealing with discontinuity was also proposed

The associate editor coordinating the review of this manuscript and approving it for publication was Xiaofan He.

recently [11]. Other researchers developed a root MUSIC method based on coprime array which can reduce the computational complexity [12]. Moreover, some types of sparse array have been designed and analyzed to meet the property of non-circular signals [13], [14]. In order to avoid the limit of ULA, this paper considers a new antenna array named as nested array which is composed of two or more uniform array with different spaces [15], [16]. Suppose that there is a two level nested linear array of $O(M)$ sensors and it can naturally resolve $O(M^2)$ DOAs of impinging sources. A spatial smoothing MUSIC scheme based on vectorization has been developed in [15] but it only discusses the circular signals. The non-circularity of impinging sources has been exploited in [17] to improve the performance of DOA estimation based on nested array. In practice, there are also many cases of mixed circular and non-circular sources. Therefore, it always makes sense to focus on DOA estimation of mixed circular and non-circular soures. Although the problem of direction finding for mixed circular and non-circular signals can be solved through method in [15] if all impinging sources are considered as circular signals, DOA estimation in presence of mixed circular and non-circular signals is still a crucial problem to address. Given that the sparse nested array has a high DOF, it is significant to investigate the classification of circular and non-circular signals and hence to utilize properties of non-circular signals well, improving the performance of DOA estimation as much as possible.

Therefore, this paper focuses on underdetermined DOA estimation of high accuracy in a mixture of circular and non-circular signals using nested array. Several algorithms under the condition of mixed circular and non-circular signals have been proposed for polarization channel estimation [18], DOA estimation of wideband signals [19], distributed sources [20], [21] and so forth. Yue *et al.* proposed a fast DOA estimation algorithm based on polynomial-rooting although the number of detectable sources is hardly satisfactory [22]. Besides, a compressive sensing (CS) based algorithm using sparse arrays [23] achieves high DOF but it introduces heavy calculation burden simultaneously. Generally, algorithms like [23], [24] using sparse array are raised to increase DOF and accuracy of estimation results. However, [24] ignores the inconsecutive parts in co-array and cannot distinguish between circular and non-circular signals which come from the same direction. Reference [25] introduces a circularity-based DOA estimation method which omits the conjugation part of elliptic covariance and hence loses DOF. It resolves DOA of circular signals using estimated DOA of non-circular signals, which will bring about error accumulation as well. Some other methods in [26]–[28] could also solve the problem of two-dimentional DOA estimation.

Solving the problem of DOA estimation in a mixture of circular and non-circular signals with high accuracy and DOF is the main concern throughout the paper. Through revision of difference and sum co-array, it can be found that circular and non-circular terms spread in entries of reconstructed Toeplitz covariance matrix respectively. The feature could also be utilized to distinguish the two types of signals and resolve the DOAs separately. Moreover, the property of non-circular signals can be fully utilized to increase both accuracy and number of identifiable sources. On the basis of former research and analysis, this paper presents the problem formulation including signal model for a mixture of circular and non-circular signals firstly. A Toeplitz covariance matrix resolving DOAs of non-circular sources is also constructed with ECM. In this process, holes in virtual array appear and a method based on matrix completion is introduced to recover the missing values in reconstructed covariance matrix, which can also increase the number of detectable sources. Moreover, based on the property mentioned earlier, we can extract circular terms from the Toeplitz matrix reconstructed by both CM and ECM with a separation technique whose feasibility is theoretically proved in Appendix.

This paper is organized as follows. In Section 2, introduction of array model for mixed circular and non-circular signals and a brief explanation about difference and sum co-array is given. Then DOA estimation of non-circular sources with matrix completion using singular value threshold (SVT) is presented in Section 3. A separation technique is also introduced to extract circular terms and get the DOAs of circular sources. Section 4 analyzes computational complexity and freedom degrees in detail. Numerical results which illustrate the efficiency of the proposed algorithm are provided in Section 5. Finally, conclusions are summarized in Section 6.

Throughout the paper, $[\bullet]^*$, $[\bullet]^T$ and $[\bullet]^H$ denote the conjunction, transpose and conjugate transpose respectively. In addition, $\| \bullet \|_*$ denotes the nuclear norm of matrix and $\| \bullet \|_F$ denotes the Frobenius norm of matrix.

II. PROBLEM FORMULATION

A. ARRAY MODEL

A two level nested array of M sensors is considered here. Assume M_1 and M_2 are the number of sensors in each level, which located along the X-axis. Without losing generality, we assume that the two level nested array has a property of $M_1 = M_2 = M/2$. Suppose that the unit inter-element spacing is $d = \lambda/2$ and λ denotes the wavelength of impinging signals. Consider K far-field narrowband sources impinging on antenna array from angles $\theta_k, k = 1, \ldots, K$. Note that the K sources are uncorrelated with each other. The received data from M sensors can be described as

$$\mathbf{X}(t) = \mathbf{A}(\theta)\mathbf{S}(t) + \mathbf{N}(t), \tag{1}$$

where $\mathbf{A}(\theta) \in \mathbb{C}^{M\times K}$ is the array manifold matrix, $\mathbf{S}(t) \in \mathbb{C}^{K\times 1}$ is the source signal vector which is composed of zero-mean wide sense stationary (WSS) signals and $\mathbf{N}(t)$ is the additive white circular complex Gaussian noise vectors with identical power σ_N^2.

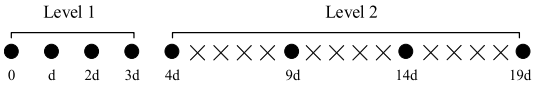

FIGURE 1. A 2 level nested array with 4 sensors in each level.

The array manifold is

$$\mathbf{A} = \begin{bmatrix} \mathbf{a}(\theta_1) & \mathbf{a}(\theta_2) & \cdots & \mathbf{a}(\theta_K) \end{bmatrix}, \tag{2}$$

where $[\mathbf{a}(\theta_k)]_i = e^{jN_i w_k}$ and $w_k = 2\pi d sin\theta_k/\lambda$. Note that $N_i d$ denotes the position of the ith sensor. Figure 1 shows the array geometry of a 2 level nested array when $M = 8$ and there are same sensors in each level.

The source signal vector is

$$\mathbf{S}(t) = \begin{bmatrix} \mathbf{s}_1(t) & \mathbf{s}_2(t) & \cdots & \mathbf{s}_K(t) \end{bmatrix}^T, \tag{3}$$

where $t = 1, 2, \ldots, T$ denotes the sampling time interval and T is the number of snapshots.

Second-order statistics of array received data, mainly covariance matrix of the received data, are mostly used to estimate θ with given time intervals of sources signals. It can be expressed as

$$\mathbf{R}_x = E[\mathbf{X}(t)\mathbf{X}^H(t)] = \mathbf{A}(\theta)\mathbf{R}_{ss}\mathbf{A}^H(\theta) + \sigma_N^2\mathbf{I}, \tag{4}$$

where $\mathbf{R}_{ss} = E[\mathbf{S}(t)\mathbf{S}^H(t)] = diag[\,\sigma_1^2\ \sigma_2^2\ \cdots\ \sigma_K^2\,]$ is the source signal covariance matrix, $\mathbf{I}$ is a unit matrix and σ_N^2 is the power of noise $\mathbf{N}(t)$. Besides, $diag[\bullet]$ denotes a diagonal matrix whose diagonal elements are the same as the vector in square brackets.

However, the number of snapshots would be always finite in practice, T for example. In this circumstance, $\mathbf{R}_x$ can be estimated with time average instead of statistical average values. Therefore,

$$\hat{\mathbf{R}}_x = \frac{1}{T}\sum_{t=1}^{T}\mathbf{X}(t)\mathbf{X}^H(t). \tag{5}$$

B. MIXED CIRCULAR AND NON-CIRCULAR SIGNALS

Circularity is an important property of random variables. In practice, there are many communication signals with QPSK and QAM modulation that have circular features and those with ASK, BPSK and UQPSK modulation, which have non-circular features. Covariance matrix is a common one for narrowband circular signals in the second orders statistical properties. Correspondingly, the elliptic covariance can also be fully exploited to improve performance of DOA estimation for non-circular signals. This paper focuses on non-circular signals such as BPSK specifically whose non-circularity rate $\rho_k = 1$, namely, strictly non-circular signals.

Assuming that there are K_c circular signals and K_n non-circular signas, with $K = K_c + K_n$. Similarly, all K impinging signals are uncorrelated with each other. Thus (3) can be rewritten as

$$\mathbf{S}(t) = \begin{bmatrix} \mathbf{s}_{c,1}(t) & \cdots & \mathbf{s}_{c,K_c}(t)\mathbf{s}_{n,1}(t) & \cdots & \mathbf{s}_{n,K_n}(t) \end{bmatrix}^T, \tag{6}$$

As it was mentioned earlier, the elliptic covariance of non-circular signals is not zero and this property can be utilized to expand the virtual array. The elliptic covariance can be used by combining $\mathbf{X}(t)$ and its conjugate counterpart as [29]

$$\mathbf{Y}(t) = \begin{bmatrix} \mathbf{X}(t) \\ \mathbf{X}^*(t) \end{bmatrix}, \tag{7}$$

According to (4), the covariance matrix can be expanded to [29]

$$\begin{aligned} \mathbf{R}_y &= E\left[\mathbf{Y}(t)\mathbf{Y}^H(t)\right] \\ &= E\begin{bmatrix} \mathbf{X}\mathbf{X}^H & \mathbf{X}\mathbf{X}^T \\ \mathbf{X}^*\mathbf{X}^H & \mathbf{X}^*\mathbf{X}^T \end{bmatrix}. \end{aligned} \tag{8}$$

In (7) and (8), the elliptic covariance matrix can extend the received data matrix and obtain a better performance when there are non-circular signals. However, we can hardly estimate all incoming signal angles through (7) in a mixture of circular and non-circular signals for the elliptic covariance of circular signals is zero. Therefore, it is helpful to separate circular and non-circular signals and estimate them respectively to get more accurate results by utilizing non-circularity, which is the focal point of this paper.

C. REVISION OF DIFFERENCE AND SUM CO-ARRAY

As it was analyzed in [15], nonuniform array such as nested array is one of key ideas behind the ability to find more sources than physical sensors because its difference co-array has considerably increased degrees of freedom. Consider a nested array whose sensors located at $L_{inner} = \{md, m = 0, 1, \ldots, M/2-1\}$ and $L_{outer} = \{(M/2+(M/2+1)n)d, n = 0, 1, \ldots, M/2-1\}$. Following [15] and [30], co-array can be generated by vectoring the covariance matrix and in (8) it turns out to be

$$\begin{aligned} \mathbf{r}_d &= vec(\mathbf{R}_y) = \sum_{k=1}^{K}\sigma_k^2\mathbf{a}_d(\theta_k) + \sigma_N^2\vec{\mathbf{1}} \\ &= \mathbf{A}_d\mathbf{p} + \sigma_N^2\vec{\mathbf{1}}, \end{aligned} \tag{9}$$

where $vec(\bullet)$ denotes vectorization, namely, rearranging entries of the matrix into a vector by column. In addition, $\mathbf{A}_d$ denotes the equivalent array manifold and $\mathbf{p}$ is the corresponding source vector. In addition, $\vec{\mathbf{1}} = [\,\mathbf{e}_1\ \mathbf{e}_2\ \cdots\ \mathbf{e}_M\,]^T$ denotes equivalent noise component, where $\mathbf{e}_i$ is a row vector with a 1 at the ith position and zeros at other positions.

$$\mathbf{p} = \begin{bmatrix} \sigma_1^2, & \ldots, & \sigma_K^2 \end{bmatrix}^T, \tag{10}$$

$$\mathbf{A}_d = [\mathbf{a}_d(\theta_1), \quad \cdots, \quad \mathbf{a}_d(\theta_K)]. \tag{11}$$

With $\otimes$ denotes the Kronecker product, the steering vectors can be expressed as

$$\mathbf{a}_d(\theta_k) = \mathbf{a}^*(\theta_k) \otimes \mathbf{a}(\theta_k), \tag{12}$$

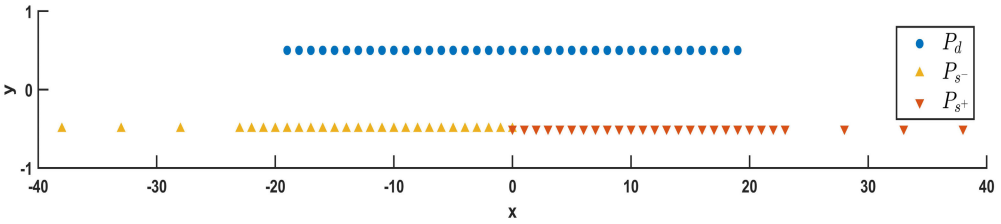

FIGURE 2. Difference and sum co-array of 8 sensors nested array when $M_1 = M_2 = 4$.

Consider about (9), $\mathbf{r}_d$ is related to difference component of co-array. According to [31], [32] about difference co-array, the location information of difference co-array can be described as

$$P_d = \left\{\vec{\mathbf{x}}_i - \vec{\mathbf{x}}_j\right\}, \quad \forall i,\ j = 0, 1, \cdots, M-1, \tag{13}$$

where $\vec{\mathbf{x}}_i$ denotes the position vector of ith elements in antenna array.

Similarly, the vector form of elliptic covariance $\mathbf{R}_{x^+} = E[\mathbf{X}\mathbf{X}^T]$ (and its conjugation $\mathbf{R}_{x^-} = E[\mathbf{X}^*\mathbf{X}^H]$) in (8) can be presented as

$$\mathbf{r}_{n^+} = vec(\mathbf{R}_{x^+}) = \sum_{k=1}^{K} \sigma_k^2 \mathbf{a}_{n^+}(\theta_k) = \mathbf{A}_{n^+}\mathbf{p}_{n^+}, \tag{14}$$

$$\mathbf{r}_{n^-} = vec(\mathbf{R}_{x^-}) = \sum_{k=1}^{K} \sigma_k^2 \mathbf{a}_{n^-}(\theta_k) = \mathbf{A}_{n^-}\mathbf{p}_{n^-}, \tag{15}$$

where

$$\mathbf{A}_{n^+} = [\mathbf{a}_{n^+}(\theta_1), \cdots, \mathbf{a}_{n^+}(\theta_K)], \tag{16}$$

$$\mathbf{A}_{n^-} = [\mathbf{a}_{n^-}(\theta_1), \cdots, \mathbf{a}_{n^-}(\theta_K)], \tag{17}$$

$$\mathbf{a}_{n^+}(\theta_k) = \mathbf{a}(\theta_k) \otimes \mathbf{a}(\theta_k), \tag{18}$$

$$\mathbf{a}_{n^-}(\theta_k) = \mathbf{a}^*(\theta_k) \otimes \mathbf{a}^*(\theta_k), \tag{19}$$

$$\mathbf{p}_{n^+} = \left[\sigma_1^2, \ldots, \sigma_K^2\right]^T, \tag{20}$$

$$\mathbf{p}_{n^-} = \left[\sigma_1^2, \ldots, \sigma_K^2\right]^T. \tag{21}$$

Accordingly, $\mathbf{r}_{n^+}$ ($\mathbf{r}_{n^-}$) is associated with sum component (and its negative) of co-array and the location of these elements can be defined as

$$P_{n^+} = \left\{\vec{\mathbf{x}}_i + \vec{\mathbf{x}}_j\right\}, \quad \forall i,\ j = 0, 1, \cdots, M-1, \tag{22}$$

$$P_{n^-} = -\left\{\vec{\mathbf{x}}_i + \vec{\mathbf{x}}_j\right\}, \quad \forall i,\ j = 0, 1, \cdots, M-1. \tag{23}$$

Figure 2 shows the location of three kinds of co-array, which indicates that non-circular case has higher array aperture and degrees of freedom than circular case. Take a two level nested array into consideration, the corresponding co-array has its elements located at nd, $-M_v \le n \le M_v$. Here $M_v = M^2/4 + M/2 - 1$ if we take P_d only and if we consider about P_{n^+} and P_{n^-}, it becomes $M^2/2 + M - 2$.

III. DOA ESTIMATION WITH ECM SEPARATION TECHNIQUE

A. DOA ESTIMATION OF NON-CIRCULAR SIGNALS

As it was introduced earlier, non-circular signals have the elliptic covariance of non-zero values while that of circular signals is zero. Therefore, we can first estimate DOA of non-circular signals by utilizing the property of elliptic covariance. In this section, the arrival angle estimation does not involve circular signals and could still enjoy the advantage of extended array aperture and DOFs.

From (22) and (23), elliptic covariance matrix $\mathbf{R}_{x^+}$ and $\mathbf{R}_{x^-}$ correspond to positive and negative components of co-array respectively. Thus we analyze them step by step and first introduce a toeplitz matrix reconstruction technique instead of conventional spatial smoothing method. According to (14), (16) and (18), there are repeated elements in $\mathbf{a}_{n^+}(\theta_k)$, which is the generator of sum co-array.

$$\mathbf{a}_{n^+}(\theta_k) = \left[\mathbf{a}(\theta_k)^T \quad \mathbf{a}(\theta_k)^T e^{jw_k} \quad \cdots \quad \mathbf{a}(\theta_k)^T e^{j(M^2/4+M/2-1)w_k}\right]^T, \tag{24}$$

where $\mathbf{a}_{n^+}(\theta_k) \in \mathbb{C}^{M^2\times 1}$.

The above studies prove that virtual sensors containing location information can be generated by (24). In fact, it is a vector which can be considered as equivalent virtual array manifold varying from 0 to $(M^2/2+M-2)d$. Direct toeplitz matrix reconstruction can be applied to nested array instead of spatial smoothing technique as a consequence. Though there are several repeated elements, we can pick up the array received data in (14) whose location is distinct from each other. Similar to $\mathbf{R}_x$ in (4), the equivalent virtual array covariance matrix has a toeplitz structure. It is of great convenience to reconstruct the covariance matrix through some distinct elements in (24) without subarray division and moving average in spatial smoothing.

Similarly, consider about (15), (17) and (19), we get

$$\mathbf{a}_{n^-}(\theta_k) = \left[\mathbf{a}(\theta_k)^H \quad \mathbf{a}(\theta_k)^H e^{-jw_k} \quad \cdots \mathbf{a}(\theta_k)^H e^{-j(M^2/4+M/2-1)w_k}\right]^T, \tag{25}$$

Combine $\mathbf{a}_{n^+}(\theta_k)$ and $\mathbf{a}_{n^-}(\theta_k)$ together, namely, (24) and (25), we establish a virtual array with sum component (and its negative). By removing the repeated elements (after their first occurrence) and then arrange them in the order of

sensor location from $(-M^2/2-M+2)d$ to $(M^2/2+M-2)d$, the new vector $\check{\mathbf{r}}_n$ of size $(M^2+2M-3)\times 1$ can be expressed as

$$\begin{aligned}\check{\mathbf{r}}_n &= \check{\mathbf{A}}_n\mathbf{p}_n \\ &= \begin{bmatrix}\check{\mathbf{A}}_{n^-} & 0 \\ 0 & \check{\mathbf{A}}_{n^+}\end{bmatrix}\begin{bmatrix}\mathbf{p}_{n^-} \\ \mathbf{p}_{n^+}\end{bmatrix}\end{aligned} \tag{26}$$

It has consecutive and inconsecutive parts as shown in Figure 2. It is to note that the missing values in the inconsecutive parts have been set to zero. Although the array aperture and DOFs have been increased under this circumstance compared to circular signals, they can be further improved by making full use of those inconsecutive parts. Therefore, a matrix completion method is employed in this section so that the whole virtual array can be fully utilized.

The equivalent covariance matrix $\check{\mathbf{R}}_n$ can be reconstructed with elements in (26), including zero values corresponding to holes in virtual array. Various matrix completion methods including Toeplitz matrix completion [33], [34] have been proposed for DOA estimation in the past few decades and most of them are used in nonuniform sparse array. In matrix completion theory, approximating matrix with rank minimization is the most popular way to fix the problem [35], [36]. Furthermore, many rank minimization problems are converted to nuclear norm minimization problem through convex relaxation. Considering about [37], Cai *et al.* has studied nuclear norm minimization problem and also derived a computational efficiency and fast converging solution called SVT to this problem. Hypothetically, $\hat{\mathbf{R}}_n$ is the unknown matrix with low rank component,

$$\begin{aligned}&min\ \rho\left\|\hat{\mathbf{R}}_n\right\|_* + \frac{1}{2}\left\|\hat{\mathbf{R}}_n\right\|_F^2 \\ &s.t.\ \left\|\mathcal{P}_\Omega(\hat{\mathbf{R}}_n) - \check{\mathbf{R}}_n\right\|_F^2 \le \epsilon,\end{aligned} \tag{27}$$

where Ω denotes a location set of all non-zero values in $\check{\mathbf{R}}_n$. As is introduced at the end of Section I, $\|\hat{\mathbf{R}}_n\|_*$ denotes nuclear norm, which equals to the sum of singular values of $\hat{\mathbf{R}}_n$. Similarly, $\|\bullet\|_F$ denotes Frobenius norm and in (27), $\|\bullet\|_F^2$ equals to the standard inner product of an arbitrary matrix. Moreover, we define an orthogonal projector $\mathcal{P}_\Omega$ which makes matrices vanishing outside of Ω. Namely, the (i,j)th element of an arbitrary matrix, $\check{\mathbf{R}}_n$ for example, is equal to $\mathcal{P}_\Omega(\check{\mathbf{R}}_n)$ if $(i,j)\in\Omega$ and the other elements of $\mathcal{P}_\Omega(\check{\mathbf{R}}_n)$ is zero. Besides, ρ denotes soft-thresholding level which is a constant and the bigger it is, the more approximate (27) is to rank minimization problem. ϵ is also a constant that depends on noise power.

It is noteworthy that the singular value thresholding algorithm, first applied in image processing, is an iteration algorithm. The initialization has been studied in [37] and according to the rules, it can be assigned as $\rho = 5(M^2/2+M-1)$, $\delta = 1.39$ and $\epsilon = 10^{-4}$ in this paper. After completion of the missing values in covariance matrix, subspace-based methods can be applied to find the angle of impinging signals. Assuming that $\hat{\mathbf{R}}_{opt}$ is the optimal solution to SVT, we can perform eigenvalue decomposition like

$$\hat{\mathbf{R}}_{opt} = \mathbf{U}_S\Sigma_S\mathbf{V}_S^H + \mathbf{U}_N\Sigma_N\mathbf{V}_N^H, \tag{28}$$

here $\mathbf{U}_S$ denotes signal subspace composed of eigenvectors corresponding to K_n large eigenvalues of $\hat{\mathbf{R}}_{opt}$, while $\mathbf{U}_N$ denotes noise subspace composed of eigenvectors corresponding to another M_n+1-K_n small eigenvalues. We assume that the source number K_n is known, which can be predicted by source number detection algorithms like minimum description length (MDL) method. Considering that the extended virtual array resulting from non-circular signals can bring higher computational complexity, we introduce the root-MUSIC to realize the fast estimation of arrival angle [38]–[40].

According to (26), the steering vector of virtual array can be expressed as

$$\check{\mathbf{a}}_n(\theta) = \begin{bmatrix}1 & e^{jw} & e^{j2w} & \cdots & e^{jM_nw}\end{bmatrix}^T, \tag{29}$$

where $w = 2\pi d sin\theta/\lambda$. Note that $z = e^{jw}$, the Z-transform of virtual array steering vector $\check{\mathbf{a}}_n(\theta)$ can be defined as

$$\check{\mathbf{a}}_n(z) = \begin{bmatrix}1 & z^1 & z^2 & \cdots & z^{M_n}\end{bmatrix}^T, \tag{30}$$

where $M_n = M^2/2+M-2$.

Based on the orthogonal relationship between virtual array steering vector and noise subspace, the root polynomial can be presented as

$$\mathbf{p}(z) = \check{\mathbf{a}}_n^H(z)\mathbf{U}_N\mathbf{U}_N^H\check{\mathbf{a}}_n(z), \tag{31}$$

here $\check{\mathbf{a}}_n(z)$ has the structure of $\check{\mathbf{a}}_n(\theta)$ and it is orthogonal to noise subspace $\mathbf{U}_N$. Besides, $\mathbf{p}(z)$ is M_n-th polynomial whose roots are symmetrical of unit circle. Note that the K_n roots with maximum amplitude in the unit circle contain information of arrival angle, thus the estimation results can be expressed as

$$\hat{\theta}_k = \arcsin\left(\frac{\lambda}{2\pi d}arg(\hat{z}_k)\right), \tag{32}$$

where $arg(\bullet)$ denotes the phase of $(\bullet)$.

B. DOA ESTIMATION OF CIRCULAR SIGNALS

After estimation of non-circular signals, a separation method can be used to extract circular components from covariance matrix and give a high precision result of circular signals. Different from estimation of non-circular signals, the covariance matrix, viz., difference co-array is considered in this section. Through analysis of sensor location and received data in covariance matrix and elliptic covariance matrix respectively, we can obtain circular and non-circular information marked by positions. Based on toeplitz matrix reconstruction, an equivalent covariance matrix containing only circular components is constructed through calculations by adding and subtracting corresponding elements.

Taking (4), (9) and (12) into account, there are also repeated sensors in $\mathbf{a}_d(\theta_k)$, which is the generator of difference co-array.

$$\mathbf{a}_d(\theta_k) = \left[\mathbf{a}(\theta_k)^T \quad \mathbf{a}(\theta_k)^T e^{-jw_k} \quad \cdots \quad \mathbf{a}(\theta_k)^T e^{-j(M^2/4+M/2-1)w_k}\right]^T, \tag{33}$$

where $\mathbf{a}_d(\theta_k) \in \mathbb{C}^{M^2\times 1}$ whose sensors location varies from $(-M^2/4 - M/2 + 1)d$ to $(M^2/4 + M/2 - 1)d$.

In (9), $\mathbf{R}_y$ includes both circular and non-circular components, so is $\mathbf{r}_d$. Most importantly, its virtual array is expanded due to property of nested array and non-circular characteristics does not work on array extension. It means that several virtual sensors in $\check{\mathbf{r}}_n$ will be omited to keep the dimension of two data vectors same.

Similarly, by removing the repeated elements in $\mathbf{r}_d$ after their first occurrence and arranging them in the order of $(-M^2/4-M/2+1)d$ to $(M^2/4+M/2-1)d$, a new data vector $\check{\mathbf{r}}_d \in \mathbb{C}^{(M^2/2+M-1)\times 1}$ can be constructed. The covariance matrix reconstructed from $\check{\mathbf{r}}_d$ is of size $M_c = M^2/4 + M/2$. Suppose p_d^i denotes the ith elements in $\check{\mathbf{r}}_d$ which represents difference co-array. Let m denotes M_c for convenience, the reconstructed covariance matrix can be defined as

$$\check{\mathbf{R}}_d = \begin{bmatrix} p_d^m & p_d^{m-1} & \cdots & p_d^1 \\ p_d^{m+1} & p_d^m & \cdots & p_d^2 \\ \vdots & \vdots & \ddots & \vdots \\ p_d^{2m-1} & p_d^{2m-2} & \cdots & p_d^m \end{bmatrix}, \tag{34}$$

here $\check{\mathbf{R}}_d$ is a $m \times m$ reconstructed covariance matrix which contains both circular and non-circular signals. As it was analyzed earlier, virtual array generated by non-circular signals is much longer than $\check{\mathbf{r}}_d$ and hence we choose the data whose corresponding virtual sensor is located from $(-M^2/4 - M/2 + 1)d$ to $(M^2/4+M/2-1)d$ in $\check{\mathbf{r}}_n$. Hence we can get a new data vector $\check{\mathbf{r}}_{ns} \in \mathbb{C}^{(2m-1)\times 1}$ which denotes array received data in a shortened virtual array.

Now, suppose that p_n^i denotes the ith elements in $\check{\mathbf{r}}_{ns}$ which represents the sum (and its negative) co-array. The reconstructed covariance matrix composed of non-circular component can be defined as

$$\check{\mathbf{R}}_{ns} = \begin{bmatrix} p_n^m & p_n^{m-1} & \cdots & p_n^1 \\ p_n^{m+1} & p_n^m & \cdots & p_m^2 \\ \vdots & \vdots & \ddots & \vdots \\ p_n^{2m-1} & p_n^{2m-2} & \cdots & p_n^m \end{bmatrix}, \tag{35}$$

where $\check{\mathbf{R}}_{ns} \in \mathbb{C}^{m\times m}$ contains only non-circular components in received data. The circular components can be extracted by subtracting (35) from (34) in theory as long as non-circular term in one equation is equal to its conterpart in another. A series of simulations and numerical results prove that the proposed ECM separation technique works well and achieves better performance than conventional methods. Besides, we shall carry out theoretical derivation and give a proof of feasibility of the separation technique in Appendix.

After separation, the covariance matrix containing only circular components can be described as

$$\hat{\mathbf{R}}_c = \check{\mathbf{R}}_d - \check{\mathbf{R}}_{ns}. \tag{36}$$

Here root-MUSIC is also utilized to give the fast estimation and avoid mass computation. Note that the total source number can be predicted through source number detection algorithms like MDL. Furthermore, we establish a covariance matrix containing only non-circular components in last section so that the number of non-circular signals can be obtained through methods like MDL. Therefore, the number of circular signals K_c can be calculated by $K_c = K - K_n$.

Similar to (29), virtual array steering vector has the form of $[\check{\mathbf{a}}_c(\theta)]_i = e^{jiw}$, where $i = 0, \cdots, m-1$ and $w = 2\pi d sin\theta/\lambda$. With $z = e^{jw}$, the Z-transform of $\check{\mathbf{a}}_c(\theta)$ can be defined as

$$\check{\mathbf{a}}_c(z) = \left[1 \quad z^1 \quad z^2 \quad \cdots \quad z^{m-1}\right], \tag{37}$$

Similarly, we can conduct eigenvalue decomposition of $\hat{\mathbf{R}}_c$ and list the eigenvalues in descending order. Supposed that the last $m - K_c$ eigenvectors constitute $\mathbf{U}'_N$, which spans the noise subspace. With the orthogonal relationship between signal subspace and noise subspace, we can obtain the root polynomial $\check{\mathbf{p}}(z)$ which is similar to (31).

$$\mathbf{p}'(z) = \check{\mathbf{a}}_c^H(z)\mathbf{U}'_N\mathbf{U}'^H_N\check{\mathbf{a}}_c(z). \tag{38}$$

Here $\mathbf{p}'(z)$ is a m-th polynomial and the K_c roots with maximum amplitude within the unit circle contain information of arrival angle, thus we can estimate the DOA with

$$\hat{\theta}'_k = \arcsin\left(\frac{\lambda}{2\pi d} arg(\hat{z}'_k)\right). \tag{39}$$

IV. COMPUTATIONAL COMPLEXITY AND FREEDOM DEGREE ANALYSIS

In this part, we concentrate on computational complexity and freedom degree analysis. Then we compare the proposed algorithm with spectral peak search method like MUSIC and other circularity-based methods. The proposed algorithm for circular signals is written as Proposed-C and Proposed-NC for non-circular signals.

A. COMPUTATIONAL COMPLEXITY ANALYSIS

When circular signals and non-circular signals coexist, method in [15] can estimate the DOAs by regarding all of them as circular signals using only CM, thus it is denoted as CM-MUSIC. The complexity of CM-MUSIC method mainly exists in three parts: calculation of covariance matrix based on time average, matrix eigenvalue decomposition and MUSIC. The complexities of them are $O(TM^2)$, $O((M^2/4 + M/2)^3)$ and $O((M^2/4 + M/2)(M^2/4 + M/2 - K)G_\theta)$ respectively. Here $G_\theta = 180/\Delta\theta + 1$ denotes the number of spectral points in peak search grid with $\Delta\theta$ represents search step. Therefore, the total complexity of CM-MUSIC method is $O(TM^2 + (M^2/4 + M/2)^3 + (M^2/4 + M/2)(M^2/4 + M/2 - K)G_\theta)$.

Method in [25] has complexity mainly existing in four parts: calculation of covariance matrix through (5), matrix

TABLE 1. Complexity comparison of different algorithms.

Algorithms	Complexity
Method in [15]	$O(TM^2 + (M^2/4 + M/2)^3 + (M^2/4 + M/2)(M^2/4 + M/2 - K)G_\theta)$
Method in [25]	$O(2TM^2 + 2M^3 + 2K_n(M^2 + 2MK_n + K_n^2) + (2M^2 - MK_c - MK_n)G_\theta)$
Proposed-C	$O(4TM^2 + (M^2/4 + M/2)^3)$
Proposed-NC	$O(4TM^2 + 2(M^2/2 + M - 1)^3 N_i + (M^2/2 + M - 1)^3)$

eigenvalue decomposition, MUSIC and calculation of covariance matrix containing circular information only. Since it estimates circular and non-circular signals respectively, first three parts are calculated twice. In general, the complexity of them are $O(2TM^2)$, $O(2M^3)$, $O(M(M - K_n)G_\theta + M(M - K_c)G_\theta)$ and $O(2K_n(M^2 + 2MK_n + K_n^2))$. Thus the total complexity is $O(2TM^2 + 2M^3 + 2K_n(M^2 + 2MK_n + K_n^2) + (2M^2 - MK_c - MK_n)G_\theta)$. Although the two methods seem simple, the spectral peak search actually costs much.

As for proposed algorithm, the common part is covariance matrix estimation based on time average whose complexity is $O(4TM^2)$. In order to separate the two kinds of signals, they will be processed respectively. For non-circular signals, the DOA estimation algorithm mainly includes calculation of covariance matrix, SVT and root-MUSIC. The corresponding complexities are $O(4TM^2)$, $O(2(M^2/2 + M - 1)^3 N_i)$ and $O((M^2/2 + M - 1)^3)$, where N_i is the iterations number. The total computational complexity of Proposed-NC is $O(4TM^2 + 2(M^2/2 + M - 1)^3 N_i + (M^2/2 + M - 1)^3)$. Given that the ECM separation technique needs non-circular components in elliptic covariance to get circular components, the Proposed-C also needs calculation of (8) to estimate DOA of circular signals. Moveover, it does not need SVT to expand the virtual array, which reduces the computational complexity. The major complexities of Proposed-C exist in calculation of covariance matrix and root-MUSIC, which are $O(4TM^2)$ and $O((M^2/4 + M/2)^3)$. Therefore, the total computational complexity of Proposed-C is $O(4TM^2 + (M^2/4 + M/2)^3)$.

Table 1 summarizes the complexity of the three algorithms. In order to express the complexity more clearly, Figure 3 shows the complexity comparison versus searching step size $\Delta\theta$. It illustrates that method in [15] has the heaviest computational burden when $\Delta\theta = 0.01°$ and the complexity of Proposed-NC is higher in other circumstances. However, the complexity of Proposed-NC mainly exists in matrix completion which could bring higher DOF. Besides, SVT is also proved to be computational efficiency while compared to other methods solving nuclear norm minimization problem [37]. Although the computational burden of these algorithms does not vary much, we can sacrifice DOF for lower complexity which abandons the use of SVT.

B. FREEDOM DEGREE ANALYSIS

Freedom degree is one of significant performance criteria in area of DOA estimation, which determines the source number of estimation. For a two level nested array with M sensors, method in [15] can only obtain freedom degrees of $O(M^2/4 + M/2)$ because it considers all impinging signals as circular signals and cannot expand the virtual array. The proposed algorithm for non-circular signals, conversely, uses elliptic covariance to reconstruct an extended virtual array covariance matrix containing only non-circular components. Hence it can acquire a higher freedom degrees of $O(M^2/2 + M - 1)$ for non-circular signals despite the coexistence. Depending on circularity, Proposed-C has a freedom degree of $O(M^2/4 + M/2)$ since it estimates circular signals without expansibility. Method in [25], also a circularity-based approach, obtains $O(M - 1)$ degrees of freedom for both circular or non-circular signals, a total of $O(2M - 2)$ degrees of freedom.

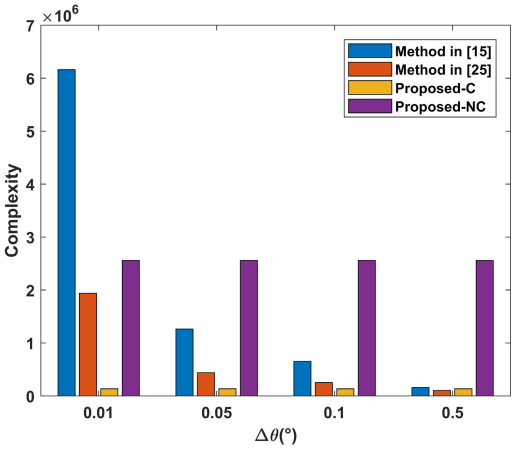

FIGURE 3. Complexity of different algorithms versus step size $\Delta\theta$.

Comparing these algorithms, we can find that the proposed algorithm not only can distinguish two kinds of signals, but also improve the detection source number and estimation performance of non-circular signals. The freedom degrees comparison is presented in Figure 4. Proposed-C has the same degree of freedom with the method in [15] as is shown in Figure 4. However, Proposed-C only resolves DOA of circular signals with up to $O(M^2/4 + M/2)$ freedom degrees while method in [15] estimates both circular and non-circular signals. In other words, Proposed-C can estimate more circular signals than method in [15] when circular and non-circular signals coexist. In conclusion, the proposed algorithm can estimate more signals than method in [15] and [25] if there are mixed circular and non-circular signals.

V. SIMULATION RESULTS

This section is intended to examine the performance of the proposed algorithm under various scenarios by comparing the proposed algorithm using SVT with the CM-MUSIC

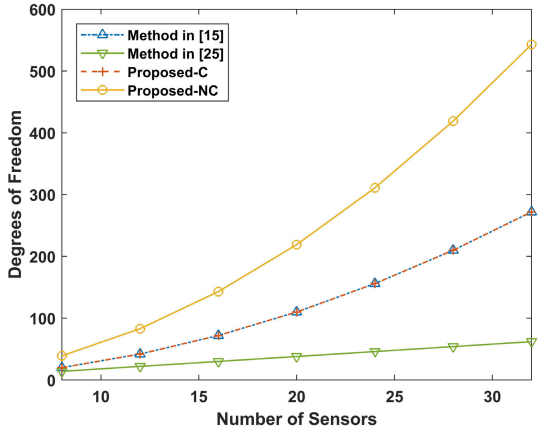

FIGURE 4. Degrees of freedom versus number of sensors.

method in [15] and a circularity-based method in [25]. It is noteworthy that method in [25] uses a uniform linear array with M sensors to conduct estimation. To assess the accuracy of them, we firstly introduce the root mean square error (RMSE), which is defined as

$$RMSE = \sqrt{\frac{1}{QK}\sum_{i=1}^{Q}\left\|\Theta - \hat{\Theta}_i\right\|^2}, \tag{40}$$

where Θ denotes the real value and $\hat{\Theta}$ is the ith estimated value. Q denotes the number of Monte Carlo simulations. Note that a two level nested linear array with $M_1 = M_2 = 4$ is employed for all experiments. For comparison, the deterministic Cramér-Rao bound (CRB) [41] is also included in this part.

Simulation 1: Performance under the condition of multiple mixed signals.

We concentrate on underdetermined DOA estimation and consider two cases where $K = 15$ and $K = 25$ sources impinge on the antenna array. It is a remarkable fact that these signals are uncorrelated with each other and all of them are strictly non-circular signals except one circular signal for both cases. The signal-to-noise ratio (SNR) and snapshots are 10 dB, $T = 500$ respectively. Besides, step size of method in [15] is set as $\Delta\theta = 0.05°$. The distribution of estimated DOAs using proposed algorithms and the spectrum of method in [15] are presented in Figure 5. In (a), it shows that both method in [15] and proposed method can find all 15 sources, which proves that the proposed method can solve DOA estimation problems in underdetermined situation. Furthermore, (b) demonstrates the fact that Proposed-NC can still resolve DOAs even when the number of non-circular signals is much larger than number of antenna array elements, improving the freedom degrees significantly. Through these figures, it shows that the proposed method using root-MUSIC has a robust performance and obtains estimated DOAs close to real values.

Simulation 2: Feasibility of proposed algorithms in a special condition.

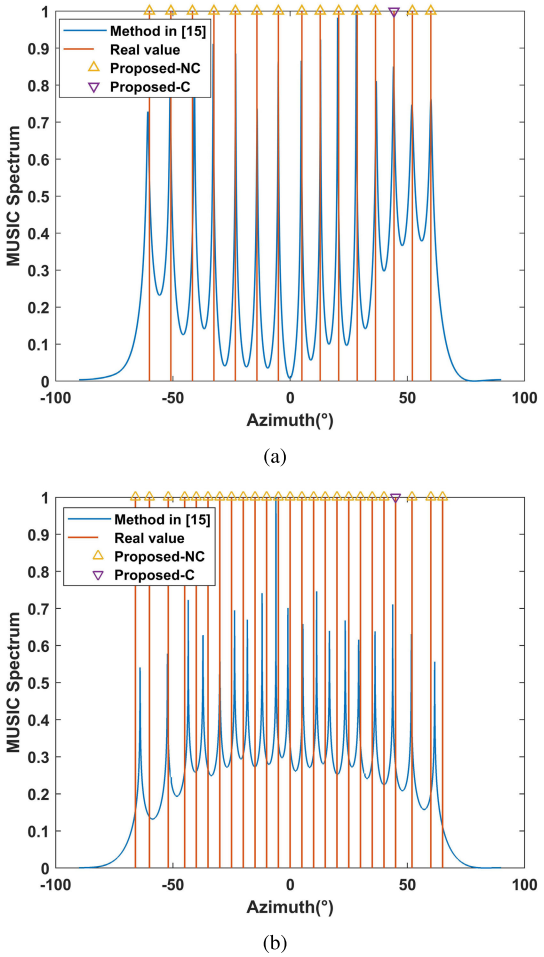

FIGURE 5. MUISC spectrum under the condition of SNR = 10dB (a) 15 sources with one circular signal; (b) 25 sources with one circular signal.

In practical application, the circular and non-circular signals may come from the same direction, thus resulting in a problem of missed detection for conventional methods. For instance, two non-circular signals with $\theta_1 = -30^o, \theta_1 = 30^o$ and a circular signal with $\theta_3 = 30^o$ are considered in set of SNR = 0 dB, $T = 500$, $\Delta\theta = 0.05°$. Since method in [15] considers all signals as circular signals, it cannot distinguish between the circular and non-circular signals from $\theta = 30^o$ so that one of impinging sources may be ignored. However, the Proposed-C and Proposed-NC estimate DOAs separately and hence they can obtain DOAs of all impinging sources despite their circularity or non-circularity. Although method in [25] can distinguish two signals from the same direction, the proposed algorithm obtains more accurate results. The results of estimation are tabulated in Table 2.

Simulation 3: RMSE comparison of the proposed algorithms, method in [15] and method in [25] versus SNR.

We conduct the simulation with Monte Carlo simulations $Q = 100$, snapshots $T = 500$ and SNRs from -5dB to 15dB with step size 5dB. Besides, the parameters are set as $K_c = 1, K_u = 2, \Delta\theta = 0.05°$ and $K_c = 1$,

TABLE 2. DOA estimation results of three methods.

method in [15]	method in [25]-C	method in [25]-NC	Proposed-C	Proposed-NC	Real value-C	Real value-NC
-29.90, 30.15	29.45	-30.35, 30.25	30.03	-29.98, 30.11	30	-30, 30

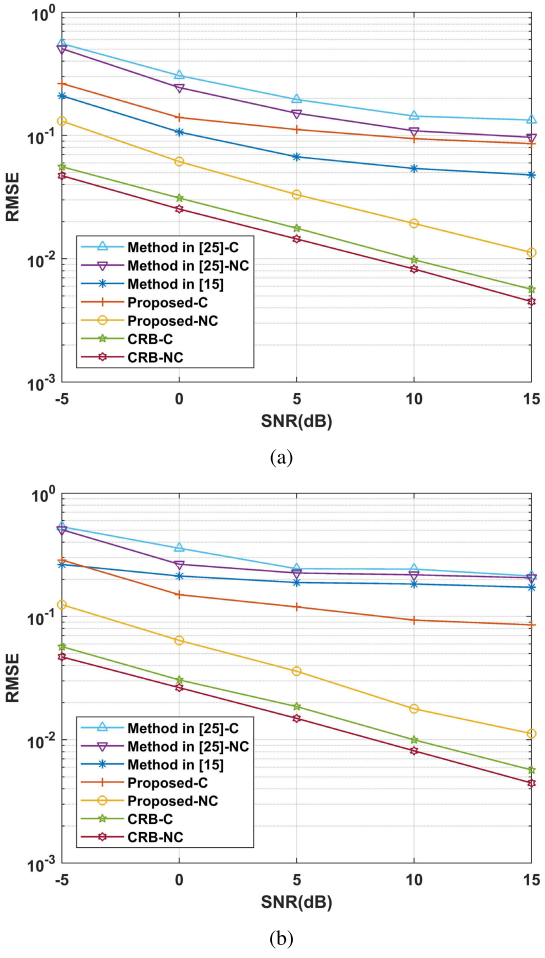

FIGURE 6. RMSE comparison under different SNRs with $D = 3$ (a) RMSE performance with $\Delta\theta = 0.05°$; (b) RMSE performance with $\Delta\theta = 0.5°$.

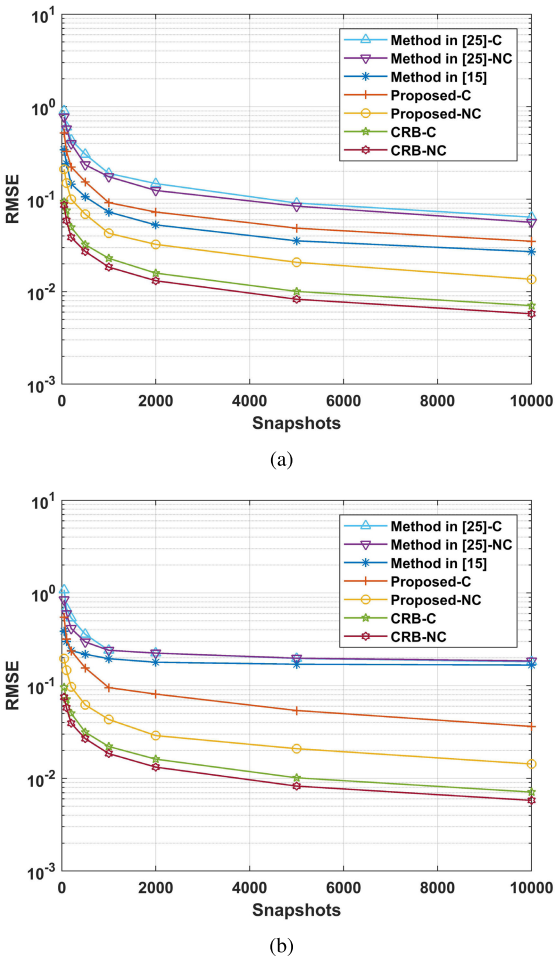

FIGURE 7. RMSE comparison under different snapshots with $D = 3$ (a) RMSE performance with $\Delta\theta = 0.05°$; (b) RMSE performance with $\Delta\theta = 0.5°$.

$K_u = 2$, $\Delta\theta = 0.5°$. It should be noted that step size mainly affects the performance of method in [15] and method in [25], which use MUSIC to resolve DOA.

In (a) of Figure 6, the step size is $\Delta\theta = 0.05°$. The proposed algorithm outperforms method in [25] in estimating circular and non-circular signals. Method in [25] only uses elliptic covariance and omits its conjugation part, thus losing array aperture and accuracy of estimation. When all impinging sources are considered as circular sources, the performance of method in [15] is slightly better than the Proposed-C, but worse than the Proposed-NC. In fact, Proposed-NC has a higher accuracy than other methods due to the extension of virtual array based on non-circular characteristics. Moreover, elliptic covariance estimated with (5) has noise components due to the finite number of snapshots. Accordingly, the error will accumulate when non-circular components are subtracted from covariance matrix of array received data and hence method in [15] outperforms Proposed-C through small searching step size at the cost of higher complexity. Consequently, Proposed-NC works better than Proposed-C due to the effect of finite number of snapshots and array extension based on non-circular characteristics.

However, error accumulation due to the finite number of snapshots is also the reason why the gap between Proposed-C and CRB-C is relatively large. (b) in Figure 6 illustrates that with $\Delta\theta = 0.5°$, the performance of method in [15] becomes worse but the complexity decreases at the same time. Hence Proposed-C offers a relatively good performance with lower calculation burden for circular signals and can detect more circular signals than method in [15] when there are both circular and non-circular signals.

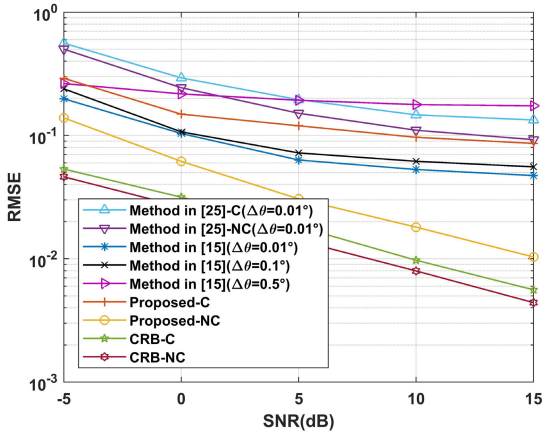

(a)

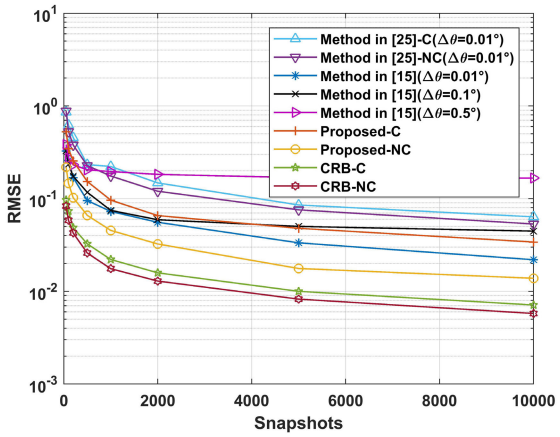

(b)

FIGURE 8. RMSE comparison under different searching step size with $D = 3$ (a) RMSE performance versus SNR with $T = 500$; (b) RMSE performance versus snapshots with $SNR = 0dB$.

Simulation 4: RMSE comparison of the proposed algorithms, method in [15] and method in [25] versus snapshots.

Simulation 4 is conducted with $SNR = 0dB$, $Q = 100$ and the number of snapshots $T = [50, 100, 200, 500, 1000, 2000, 5000, 10000]$ to study the impact of snapshots on DOA estimation. (a) and (b) in Figure 7 show the results of the three methods in set of $\Delta\theta = 0.05°$ and $\Delta\theta = 0.5°$ respectively. The Proposed-C performs slightly worse than method in [15] in small snapshots when $\Delta\theta = 0.05°$. In this circumstance, estimation of covariance through (5) introduces error due to small snapshots thus the situation getting worse after processing of separation. Method in [25] performs worse than other methods due to its small array aperture, which is similar to the conclusions in Simulation 3.

Simulation 5: RMSE comparison of the proposed algorithms, method in [15] and method in [25] under different searching step size.

In this part, several simulations have been done to study the effect of step size $\Delta\theta$ on RMSE. Assuming that $\Delta\theta = [0.01°, 0.1°, 0.5°]$, RMSE comparison versus SNR and snapshots is shown in Figure 8. It illustrates that step size $\Delta\theta$ has an important influence on performance of method in [15] and method in [25]. Large number of snapshots can decrease the error due to elliptic covariance estimation using (5). Furthermore, Proposed-C outperforms method in [15] when number of snapshots is large according to (b) in Figure 8, which confirms the conclusion of error accumulation in Simulation 3. The proposed algorithm works better than method in [25] even when $\Delta\theta = 0.01°$.

VI. CONCLUSION

The underdetermined DOA estimation in presence of mixed circular and non-circular signals is considered throughout the paper, and an ECM-based algorithm is proposed to cope with this problem. The proposed algorithm has three significant advantages. Firstly, it can detect more circular sources than number of sensors by utilizing nested array, which is extended further by SVT for non-circular sources so that more non-circular signals can be estimated than circular ones. Secondly, the proposed algorithm can estimate non-circular signals more accurately and obtain better performance than other circularity-based method like [25]. Finally, the proposed algorithm can distinguish between circular and non-circular signals, thus it can identify two signals in a special situation if circular and non-circular signals come from the same direction, while method in [15] cannot identify them. The proof of feasibility of the separation technique is given in Appendix and numerical results are presented to validate the conclusions above. Besides, the idea of separating circular and non-circular signals using elliptic covariance in this paper can also be applied to solving the problem of DOA estimation for other sparse arrays.

APPENDIX
THE FEASIBILITY OF SEPARATION TECHNIQUE

Theorem 1: When there are both circular and non-circular signals impinging on the antenna array, the reconstructed covariance matrix has exactly the same terms as those in reconstructed elliptic covariance matrix. Then, there are same terms in (34) and (35). Specifically, p_n^i, which denotes non-circular components, is one part of p_d^i. And hence $\hat{\mathbf{R}}_c$ only has circular components.

Proof: We first consider covariance matrix $\mathbf{R}_x = E[\mathbf{X}(t)\mathbf{X}^H(t)]$.

$$\begin{aligned}\mathbf{R}_x &= E[\mathbf{X}(t)\mathbf{X}^H(t)] \\ &= E[(\mathbf{AS}+\mathbf{N})(\mathbf{AS}+\mathbf{N})^H] \\ &= \mathbf{A}\mathbf{R}_s\mathbf{A}^H + \mathbf{N}\mathbf{N}^H, \end{aligned} \tag{41}$$

where $\mathbf{N}\mathbf{N}^H = \sigma^2\mathbf{I}$ and $\mathbf{I}$ is a diagonal matrix with all diagonal elements being 1. Consider about (2) and rewrite it as

$$\mathbf{A} = \begin{bmatrix}\mathbf{a}_{c_1} & \cdots & \mathbf{a}_{c_{K_c}} & \mathbf{a}_{n_1} & \cdots & \mathbf{a}_{n_{K_n}}\end{bmatrix}, \tag{42}$$

here we divide $\mathbf{A}$ into two kind of steering vectors—circular and non-circular.

Similarly, we have a new expression of $\mathbf{R}_{ss}$ according to (6).

$$\begin{aligned}\mathbf{R}_{ss} &= E[\mathbf{S}(t)\mathbf{S}^H(t)] \\ &= diag\begin{bmatrix}\sigma_{c_1}^2 & \cdots & \sigma_{c_{K_c}}^2 & \sigma_{n_1}^2 & \cdots & \sigma_{n_{K_n}}^2\end{bmatrix}. \quad (43)\end{aligned}$$

Thus (41) can be rewritten as

$$\begin{aligned}\mathbf{R}_x = \sigma_{c_1}^2\mathbf{a}_{c_1}\mathbf{a}_{c_1}^H + \cdots + \sigma_{c_1}^2\mathbf{a}_{c_{K_c}}\mathbf{a}_{c_{K_c}}^H \\ +\sigma_{n_1}^2\mathbf{a}_{n_1}\mathbf{a}_{n_1}^H + \cdots + \sigma_{n_{K_n}}^2\mathbf{a}_{n_{K_n}}\mathbf{a}_{n_{K_n}}^H. \quad (44)\end{aligned}$$

Take $\mathbf{a}_{n_1}$ as an example and according to the definition of array steering vector under (2), we can get

$$\mathbf{a}_{n_1} = \begin{bmatrix}1 & e^{jw_{n_1}} & \cdots & e^{j(M^2/4+M/2-1)w_{n_1}}\end{bmatrix}^T, \quad (45)$$

where $w_{n_1} = 2\pi dsin\theta_{n,1}/\lambda$. Then

$$\mathbf{a}_{n_1}\mathbf{a}_{n_1}^H = \begin{bmatrix} L_{n_1}^0 & L_{n_1}^{-1} & \cdots & L_{n_1}^{-(m-1)} \\ L_{n_1}^1 & L_{n_1}^0 & \cdots & L_{n_1}^{-(m-1)+1} \\ \vdots & \vdots & \ddots & \vdots \\ L_{n_1}^{m-1} & L_{n_1}^{m-2} & \cdots & L_{n_1}^0 \end{bmatrix}, \quad (46)$$

where $m = M^2/4 + M/2$. For $L_b^a = e^{j2\pi adsin\theta_b/\lambda}$, subscript $_b$ denotes the signals and superscript ^{a} denotes the location of corresponding sensors, which is the same as the terms in front of w_k. No matter it is circular or non-circular signals, we can always derive (46) from covariance matrix. Let $\mathcal{L}^a$ denotes the corresponding elements in (44), it can be defined as

$$\mathcal{L}^a = \sum_b \sigma_b^2 L_b^a, \quad b \in \{c_1, \cdots, c_{K_c}, n_1, \cdots, n_{K_n}\}. \quad (47)$$

Therefore, we can obtain (9) and (12) from (44) and (46). And $\check{\mathbf{r}}_d$, which is the vector form of distinct elements in (12), can be expressed as

$$\check{\mathbf{r}}_d = \begin{bmatrix}\mathcal{L}^{-(m-1)} & \cdots & \mathcal{L}^0 & \cdots & \mathcal{L}^{m-1}\end{bmatrix}^T. \quad (48)$$

Hence we can use (48) to reconstruct a equivalent covariance matrix based on toeplitz rules, which can be presented as

$$\check{\mathbf{R}}_d = \begin{bmatrix} \mathcal{L}^0 & \mathcal{L}^{-1} & \cdots & \mathcal{L}^{-(m-1)} \\ \mathcal{L}^1 & \mathcal{L}^0 & \cdots & \mathcal{L}^{-(m-1)+1} \\ \vdots & \vdots & \ddots & \vdots \\ \mathcal{L}^{m-1} & \mathcal{L}^{m-2} & \cdots & \mathcal{L}^0 \end{bmatrix}. \quad (49)$$

That is to say, p_d^i is the ith element in (48) and $p_d^m = \mathcal{L}^0$.

Then, we take elliptic covariance $\mathbf{R}_{x^+} = E[\mathbf{X}\mathbf{X}^T]$ (and its conjugation $\mathbf{R}_{x^-} = E[\mathbf{X}^*\mathbf{X}^H]$) into consideration. Since the complex Gaussian noise has circular characteristics, its elliptic covariance also equals zero. Therefore, $\mathbf{R}_{x^+}$ can be defined as

$$\begin{aligned}\mathbf{R}_{x^+} &= E[\mathbf{X}(t)\mathbf{X}^T(t)] \\ &= E[(\mathbf{AS}+\mathbf{N})(\mathbf{AS}+\mathbf{N})^T] \\ &= \mathbf{ASS}^T\mathbf{A}^T. \quad (50)\end{aligned}$$

Considering that the impinging sources contain both circular and non-circular signals, utilize the property of non-circular signals and we can get

$$\begin{aligned}\mathbf{R}_{s^+} &= E[\mathbf{SS}^T] \\ &= diag[0 \ \cdots \ 0 \ \sigma_{n_1}^2 \ \cdots \ \sigma_{n_{K_n}}^2]. \quad (51)\end{aligned}$$

In this circumstance, (50) can be converted to

$$\mathbf{R}_{x^+} = 0 + \cdots + 0 + \sigma_{n_1}^2\mathbf{a}_{n_1}\mathbf{a}_{n_1}^T + \cdots + \sigma_{n_{K_n}}^2\mathbf{a}_{n_{K_n}}\mathbf{a}_{n_{K_n}}^T. \quad (52)$$

Similar to (45) and (46), we first analyze $\mathbf{a}_{n_1}$ and hence

$$\mathbf{a}_{n_1}\mathbf{a}_{n_1}^T = \begin{bmatrix} L_{n_1}^0 & L_{n_1}^1 & \cdots & L_{n_1}^{m-1} \\ L_{n_1}^1 & L_{n_1}^2 & \cdots & L_{n_1}^m \\ \vdots & \vdots & \ddots & \vdots \\ L_{n_1}^{m-1} & L_{n_1}^m & \cdots & L_{n_1}^{2m-2} \end{bmatrix}. \quad (53)$$

Apply the same process to $\mathbf{R}_{x^-} = E[\mathbf{X}^*\mathbf{X}^H]$, we can get

$$\begin{aligned}\mathbf{R}_{x^-} &= E[\mathbf{X}(t)^*\mathbf{X}^H(t)] \\ &= E[(\mathbf{AS}+\mathbf{N})^*(\mathbf{AS}+\mathbf{N})^H] \\ &= (\mathbf{ASS}^T\mathbf{A}^T)^*. \quad (54)\end{aligned}$$

Note that $\mathbf{R}_{s^-} = E[\mathbf{S}^*(t)\mathbf{S}^H(t)^H]$, we can find the following results from (42) and (54)

$$\begin{aligned}\mathbf{R}_{x^-} = 0 + \cdots + 0 + \sigma_{n_1}^2\mathbf{a}_{n_1}^*\mathbf{a}_{n_1}^H + \cdots \\ +\sigma_{n_{K_n}}^2\mathbf{a}_{n_{K_n}}^*\mathbf{a}_{n_{K_n}}^H. \quad (55)\end{aligned}$$

According to (45), we can obtain

$$\mathbf{a}_{n_1}^*\mathbf{a}_{n_1}^H = \begin{bmatrix} L_{n_1}^0 & L_{n_1}^{-1} & \cdots & L_{n_1}^{-(m-1)} \\ L_{n_1}^{-1} & L_{n_1}^{-2} & \cdots & L_{n_1}^{-m} \\ \vdots & \vdots & \ddots & \vdots \\ L_{n_1}^{-(m-1)} & L_{n_1}^{-m} & \cdots & L_{n_1}^{-(2m-2)} \end{bmatrix}. \quad (56)$$

Think over (53) and (56) and we can find that they compose a complete virtual array located from $-(M^2/2+M-2)d$ to $(M^2/2+M-2)d$. It is a remarkable fact that there are some elements missing in it. Let $\tilde{\mathcal{L}}^a$ denotes the corresponding elements in (53) and (54), it can be defined as

$$\tilde{\mathcal{L}}^a = \sum_b \sigma_b^2 L_b^a, \quad b \in \{n_1, \cdots, n_{K_n}\}. \quad (57)$$

In Section 3, we remove the repeated elements in sum (and its negative) co-array after their first appearance and rearrange them to get the vector $\check{\mathbf{r}}_n$. Now, we rewrite it as

$$\check{\mathbf{r}}_n = \begin{bmatrix}\mathcal{L}^{-(2m-2)} & \cdots & \mathcal{L}^0 & \cdots & \mathcal{L}^{2m-2}\end{bmatrix}^T. \quad (58)$$

To match the length of difference co-array, we choose the corresponding sensors and get a new data vector $\check{\mathbf{r}}_{ns}$ in a shortened virtual array

$$\check{\mathbf{r}}_{ns} = \begin{bmatrix}\mathcal{L}^{-(m-1)} & \cdots & \mathcal{L}^0 & \cdots & \mathcal{L}^{m-1}\end{bmatrix}^T. \quad (59)$$

Thus, (59) can be used to reconstruct a equivalent covariance matrix for sum co-array. And it can be presented as

$$\breve{\mathbf{R}}_{ns} = \begin{bmatrix} \tilde{\mathcal{L}}^{0} & \tilde{\mathcal{L}}^{-1} & \cdots & \tilde{\mathcal{L}}^{-(m-1)} \\ \tilde{\mathcal{L}}^{1} & \tilde{\mathcal{L}}^{0} & \cdots & \tilde{\mathcal{L}}^{-(m-1)+1} \\ \vdots & \vdots & \ddots & \vdots \\ \tilde{\mathcal{L}}^{m-1} & \tilde{\mathcal{L}}^{m-2} & \cdots & \tilde{\mathcal{L}}^{0} \end{bmatrix}. \tag{60}$$

Now, consider about (36), we can find that $\hat{\mathbf{R}}_c$ equals to (49) minus (60). Moreover, it can be converted to subtraction of elements in matrix. Namely, (47) minus (57).

$$\begin{aligned} \breve{\mathcal{L}}^{a} &= \mathcal{L}^{a} - \tilde{\mathcal{L}}^{a} \\ &= \sum_{b} \sigma_b^2 L_b^a, \quad b \in \{c_1, \cdots, c_{K_c}\}. \end{aligned} \tag{61}$$

That is to say (61) only has circular components, so is $\hat{\mathbf{R}}_c$.

$$\hat{\mathbf{R}}_c = \begin{bmatrix} \breve{\mathcal{L}}^{0} & \breve{\mathcal{L}}^{-1} & \cdots & \breve{\mathcal{L}}^{-(m-1)} \\ \breve{\mathcal{L}}^{1} & \breve{\mathcal{L}}^{0} & \cdots & \breve{\mathcal{L}}^{-(m-1)+1} \\ \vdots & \vdots & \ddots & \vdots \\ \breve{\mathcal{L}}^{m-1} & \breve{\mathcal{L}}^{m-2} & \cdots & \breve{\mathcal{L}}^{0} \end{bmatrix}. \tag{62}$$

■

REFERENCES

[1] H. Krim and M. Viberg, "Two decades of array signal processing research: The parametric approach," *IEEE Signal Process. Mag.*, vol. 13, no. 4, pp. 67–94, Jul. 1996.

[2] Y. Wang, Y. Wu, and Y. Shen, "Joint spatiotemporal multipath mitigation in large-scale array localization," *IEEE Trans. Signal Process.*, vol. 67, no. 3, pp. 783–797, Feb. 2019.

[3] Y. Han, Y. Shen, X.-P. Zhang, M. Z. Win, and H. Meng, "Performance limits and geometric properties of array localization," *IEEE Trans. Inf. Theory*, vol. 62, no. 2, pp. 1054–1075, Feb. 2016.

[4] R. Schmidt, "Multiple emitter location and signal parameter estimation," *IEEE Trans. Antennas Propag.*, vol. 34, no. 3, pp. 276–280, Mar. 1986.

[5] R. Roy and T. Kailath, "ESPRIT-estimation of signal parameters via rotational invariance techniques," *IEEE Trans. Acoust., Speech, Signal Process.*, vol. 37, no. 7, pp. 984–995, Jul. 1989.

[6] S. Marcos, A. Marsal, and M. Benidir, "The propagator method for source bearing estimation," *Signal Process.*, vol. 42, no. 2, pp. 121–138, Mar. 1995.

[7] P. Gupta and M. Agrawal, "DOA estimation of non-circular signals using fourth order cumulant in underdetermined cases," in *Proc. IEEE Int. Workshop Signal Process. Syst. (SiPS)*, Oct. 2018, pp. 25–30.

[8] Y. Wang, M. Trinkle, and B. W.-H. Ng, "Efficient DOA estimation of noncircular signals in the presence of multipath propagation," *Signal Process.*, vol. 149, pp. 14–26, Aug. 2018.

[9] F. Wen, Z. Zhang, K. Wang, G. Sheng, and G. Zhang, "Angle estimation and mutual coupling self-calibration for ULA-based bistatic MIMO radar," *Signal Process.*, vol. 144, pp. 61–67, Mar. 2018.

[10] Z. Shi, C. Zhou, Y. Gu, N. A. Goodman, and F. Qu, "Source estimation using coprime array: A sparse reconstruction perspective," *IEEE Sensors J.*, vol. 17, no. 3, pp. 755–765, Feb. 2017.

[11] C. Zhou, Y. Gu, X. Fan, Z. Shi, G. Mao, and Y. D. Zhang, "Direction-of-Arrival estimation for coprime array via virtual array interpolation," *IEEE Trans. Signal Process.*, vol. 66, no. 22, pp. 5956–5971, Nov. 2018.

[12] J. Li, D. Li, D. Jiang, and X. Zhang, "Extended-aperture unitary root MUSIC-based DOA estimation for coprime array," *IEEE Commun. Lett.*, vol. 22, no. 4, pp. 752–755, Apr. 2018.

[13] P. Gupta and M. Agrawal, "Design and analysis of the sparse array for DoA estimation of noncircular signals," *IEEE Trans. Signal Process.*, vol. 67, no. 2, pp. 460–473, Jan. 2019.

[14] Y.-K. Zhang, H.-Y. Xu, D.-M. Wang, B. Ba, and S.-Y. Li, "A novel designed sparse array for noncircular sources with high degree of freedom," *Math. Problems Eng.*, vol. 2019, pp. 1–10, Jan. 2019.

[15] P. Pal and P. P. Vaidyanathan, "Nested arrays: A novel approach to array processing with enhanced degrees of freedom," *IEEE Trans. Signal Process.*, vol. 58, no. 8, pp. 4167–4181, Aug. 2010.

[16] P. Pal and P. P. Vaidyanathan, "Nested arrays in two dimensions, part I: Geometrical considerations," *IEEE Trans. Signal Process.*, vol. 60, no. 9, pp. 4694–4705, Sep. 2012.

[17] J. Zhao, S. Liu, S. Que, Q. Zou, and M. Ou, "Doa estimation for non-circular signal with nested array," *Prog. Electromagn. Res. M*, vol. 86, pp. 39–47, Sep./Oct. 2019.

[18] X. Wang, L. Wan, M. Huang, C. Shen, and K. Zhang, "Polarization channel estimation for circular and non-circular signals in massive MIMO systems," *IEEE J. Sel. Topics Signal Process.*, vol. 13, no. 5, pp. 1001–1016, Sep. 2019.

[19] Y. Huang, Y. Xu, Y. Lu, and Z. Liu, "Aligned propagator scanning approach to DOA estimation of circular and noncircular wideband source signals," *IEEE Trans. Veh. Technol.*, vol. 68, no. 2, pp. 1702–1717, Feb. 2019.

[20] Z. Huang, X. Li, P. Huang, and W. Wang, "2-D DOA estimation for incoherently distributed sources considering mixed circular and noncircular signals in massive MIMO system," *IEEE Access*, vol. 7, pp. 106900–106911, 2019.

[21] L. Wan, G. Han, J. Jiang, J. J. P. C. Rodrigues, N. Feng, and T. Zhu, "DOA estimation for coherently distributed sources considering circular and noncircular signals in massive MIMO systems," *IEEE Syst. J.*, vol. 11, no. 1, pp. 41–49, Mar. 2017.

[22] Y. Yue, Y. Xu, L. Shen, and Z. Liu, "Parameter estimation of coexisted circular and strictly non-circular signals," *Electron. Lett.*, vol. 53, no. 13, pp. 864–866, Jun. 2017.

[23] J. Cai, W. Liu, R. Zong, and B. Wu, "Sparse array extension for non-circular signals with subspace and compressive sensing based DOA estimation methods," *Signal Process.*, vol. 145, pp. 59–67, Apr. 2018.

[24] B. Li, Y. Ding, and Y. Wang, "Direction-of-arrival estimation using co-prime array in the context of both circular and non-circular sources," in *Proc. 5th Sino-French Workshop Inf. Commun. Technol. (SIFWICT)*, 2019, pp. 1–6.

[25] A. Liu, G. Liao, Q. Xu, and C. Zeng, "A circularity-based DOA estimation method under coexistence of noncircular and circular signals," in *Proc. IEEE Int. Conf. Acoust., Speech Signal Process. (ICASSP)*, Mar. 2012, pp. 2561–2564.

[26] H. Chen, C. Hou, W. Liu, W.-P. Zhu, and M. N. S. Swamy, "Efficient two-dimensional Direction-of-Arrival estimation for a mixture of circular and noncircular sources," *IEEE Sensors J.*, vol. 16, no. 8, pp. 2527–2536, Apr. 2016.

[27] H. Chen, C. Hou, W.-P. Zhu, W. Liu, Y.-Y. Dong, Z. Peng, and Q. Wang, "ESPRIT-like two-dimensional direction finding for mixed circular and strictly noncircular sources based on joint diagonalization," *Signal Process.*, vol. 141, pp. 48–56, Dec. 2017.

[28] Y. Liu, H. Chen, Z. Peng, and J. Fang, "DOA estimation for mixed circular and noncircular signals by using the conversion relationship between URAs and a virtual ULA," *IEEE Sensors Lett.*, vol. 3, no. 11, pp. 1–4, Nov. 2019.

[29] H. Abeida and J.-P. Delmas, "MUSIC-like estimation of direction of arrival for noncircular sources," *IEEE Trans. Signal Process.*, vol. 54, no. 7, pp. 2678–2690, Jul. 2006.

[30] W.-K. Ma, T.-H. Hsieh, and C.-Y. Chi, "DOA estimation of quasi-stationary signals via Khatri-Rao subspace," in *Proc. IEEE Int. Conf. Acoust., Speech Signal Process.*, Apr. 2009, pp. 2165–2168.

[31] R. T. Hoctor and S. A. Kassam, "The unifying role of the coarray in aperture synthesis for coherent and incoherent imaging," *Proc. IEEE*, vol. 78, no. 4, pp. 735–752, Apr. 1990.

[32] R. J. Kozick and S. A. Kassam, "Coarray synthesis with circular and elliptical boundary arrays," *IEEE Trans. Image Process.*, vol. 1, no. 3, pp. 391–405, Jul. 1992.

[33] Y. I. Abramovich, N. K. Spencer, and A. Y. Gorokhov, "Positive-definite Toeplitz completion in DOA estimation for nonuniform linear antenna arrays. II. Partially augmentable arrays," *IEEE Trans. Signal Process.*, vol. 47, no. 6, pp. 1502–1521, Jun. 1999.

[34] H. Huang, Y. Miao, Y. Gong, and B. Liao, "Toeplitz matrix completion for direction finding using a modified nested linear array," in *Proc. IEEE Int. Conf. Acoust., Speech Signal Process. (ICASSP)*, May 2019, pp. 4474–4478.

[35] E. J. Candès and B. Recht, "Exact matrix completion via convex optimization," *Found. Comput. Math.*, vol. 9, no. 6, p. 717, Dec. 2009.

[36] M. Fazel, H. Hindi, and S. P. Boyd, "Log-det heuristic for matrix rank minimization with applications to hankel and Euclidean distance matrices," in *Proc. Amer. Control Conf.*, vol. 3, 2003, pp. 2156–2162.
[37] J.-F. Cai, E. J. Candès, and Z. Shen, "A singular value thresholding algorithm for matrix completion," *SIAM J. Optim.*, vol. 20, no. 4, pp. 1956–1982, Jan. 2010.
[38] D. Zhang, Y. Zhang, G. Zheng, C. Feng, and J. Tang, "Improved DOA estimation algorithm for co-prime linear arrays using root-MUSIC algorithm," *Electron. Lett.*, vol. 53, no. 18, pp. 1277–1279, Aug. 2017.
[39] F.-G. Yan, L. Shuai, J. Wang, J. Shi, and M. Jin, "Real-valued root-MUSIC for DOA estimation with reduced-dimension EVD/SVD computation," *Signal Process.*, vol. 152, pp. 1–12, Nov. 2018.
[40] B. D. Rao and K. V. S. Hari, "Performance analysis of root-music," *IEEE Trans. Acoust., Speech, Signal Process.*, vol. 37, no. 12, pp. 1939–1949, Dec. 1989.
[41] J. Steinwandt, F. Roemer, and M. Haardt, "Deterministic Cramér–Rao bound for a mixture of circular and strictly non-circular signals," in *Proc. Int. Symp. Wireless Commun. Syst. (ISWCS)*, Aug. 2015, pp. 661–665.

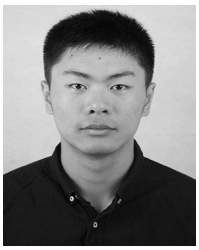

PENG HAN received the B.S. degree from the National Digital Switching System Engineering and Technological Research Center (NDSC), Zhengzhou, China, in 2017, where he is currently pursuing the M.S. degree in communications and information system. His main research interests include wireless communication theory, signal processing, and parameter estimation.

HAIYUN XU received the M.S. degree from the National Digital Switching System Engineering and Technological Research Center (NDSC), Zhengzhou, China, in June 2019, where he is currently pursuing the Ph.D. degree in communications and information system. His main research interests include wireless communication theory, signal processing, and parameter estimation.

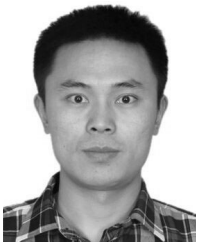

BIN BA received the M.S. and Ph.D. degrees from the National Digital Switching System Engineering and Technological Research Center (NDSC), Zhengzhou, China, in June 2012 and June 2015, respectively. He is currently working in communications and information system with NDSC. His main research interests include wireless communication theory, signal processing, and parameter estimation.

YANKUI ZHANG received the M.S. degree from the National Digital Switching System Engineering and Technological Research Center (NDSC), Zhengzhou, China, in June 2016, where he is currently pursuing the Ph.D. degree in communications and information system. His main research interests include array signal processing and parameter estimation.